MATHEMATICAL MODELING OF COMPETITION FOR LIGHT AND NUTRIENTS BETWEEN PHYTOPLANKTON SPECIES IN A POORLY MIXED WATER COLUMN

by

Thomas Stojsavljevic

A Thesis Submitted in

Partial Fulfillment of the

Requirements for the Degree of

Master of Science

in Mathematics

at

The University of Wisconsin-Milwaukee

May 2014

ABSTRACT

MATHEMATICAL MODELING OF COMPETITION FOR LIGHT AND NUTRIENTS BETWEEN PHYTOPLANKTON SPECIES IN A POORLY MIXED WATER COLUMN

by

Thomas Stojsavljevic

The University of Wisconsin-Milwaukee, 2014
Under the Supervision of Professor Gabriella Pinter

Phytoplankton live in a complex environment with two essential resources forming various gradients. Light supplied from above is never homogeneously distributed in a body of water due to refraction and absorption from biomass present in the ecosystem and from other sources. Nutrients in turn are typically supplied from below. In poorly mixed water columns phytoplankton can be heterogeneously distributed forming various layering patterns. The relationship between the location and the thickness of the layers is an open problem of interest. Here we present three models which study how competition for light and resources can form common layering patterns seen in nature and investigate how the location and thickness of the layer changes when the motility of the phytoplankton is varied. Using this we study the phenomenon of coexistence of multiple phytoplankton species and the presence of species spatial separation.

TABLE OF CONTENTS

LIST OF FIGURES

LIST OF TABLES

ACKNOWLEDGMENTS

First I wish to thank Dr. Pinter for all her insights and support in this project. Your commitment to student success and the clarity of your work will continue to serve as an influence in my future studies and career. I would also like to thank my committee members Professor Lauko and Professor Hinow for their interest in this project and taking their time to review this thesis. Finally, I would like to thank my family and friends. In particular I would like to thank Rachel Elizabeth TeWinkel for helping me format my thesis.

1 Introduction

Phytoplankton constitute an important part of aquatic ecosystems. In addition to serving as the base of the aquatic food chain, phytoplankton generate 70% of the world's atmospheric oxygen and also absorb half of the carbon dioxide contributing to global warming [2], [16]. Excessive algal growth in lakes and water reservoirs also present social and economic challenges. Besides negatively impacting water-based recreation, cases of human illness and animal deaths caused by cyanotoxins produced by certain harmful phytoplankton species have been reported. In one instance, 53 dialysis patients in Brazil died in 1996 as a result of receiving water intravenously containing high concentrations of a toxin produced by *Microcystis* [6]. Considering their wide ranging impacts it is critically important to understand the underlying dynamics of phytoplankton ecology.

In general, phytoplankton are regarded as the community of plants adapted to suspension in the sea or in fresh waters and which is susceptible to passive movement by wind and current. These include algae, diatoms, and cyanobacteria (commonly referred to as blue-green algae). Phytoplankton come in a variety of sizes and morphology which help them compete for resources such as light and nutrients [6]. From laboratory experiments, it is known that phytoplankton require inorganic nitrogen, sulphur, and phosphorous compounds along with trace elements and vitamins. For freshwater environments, phosphorus and nitrogen are often nutrients present in low amounts and inhibit biomass growth. In particular, free phosphorus is available only from geochemical sources within aquatic ecosystems [10]. Thus there are naturally occurring resource gradients where there is a larger concentration of nutrients at the bottom of a body of water than there is at the surface.

In order for algal cells to survive there needs to be a balance between light and their internal nutrients to properly conduct photosynthesis. Light is never homoge-

neously distributed in aquatic environments since it forms a gradient over biomass and other light-absorbing substances [8], [9]. The deeper a species is in the water column, the less light there is available for it to use due to the shading from populations above. Therefore spatial heterogeneity, both horizontally and vertically, created by the species throughout the environment is a key feature to understanding algal populations[11], [14], [16].

Given that light and nutrients both limit phytoplankton growth, in order to understand phytoplankton dynamics it is necessary to know how phytoplankton are able to remain suspended in the illuminated layers of the water. Continuous residence in the illuminated layers is neither necessary nor optimal for growth [18]. Since there is a wide array of phytoplankton morphology, there are several strategies employed by species in order to regulate their position. Certain species possess flagella which can be used for swimming while other species use their internal nutrients to change their buoyancy by reducing their sinking velocity in nutrient-rich water [11]. This way the effects of the light and nutrient gradients can be balanced and growth can occur.

While phytoplankton are able to regulate their location within a body of water via active movement, the physical processes caused by mixing significantly impact how phytoplankton grow. Since the phytoplankton are suspended in water and are susceptible to diffusion processes, mixing conditions produce different populations distributions vertically in a body of water. Prominent vertical distributions include deep chlorophyll maxima (DCMs), benthic layers, and surface scums [11], [14]. Deep chlorophyll maxima is the layering phenomenon where biomass accumulation happens beneath the surface of the water column. Surface scums is the layering pattern where up to 90% of the biomass concentration is near the surface resulting in heavy shading of the water. Benthic layers occur in stratified bodies of water. Stratification in bodies of water is due to temperature fluxes at the surface and advections within the body of water. The thickness of these layers is controlled by the degree of mixing and

can vary from several centimetres to tens of meters [11].

Various mathematical models have been developed to describe the dynamics of phytoplankton populations [2], [6], [11], [14], [15]. In this paper we first describe the model given in [11]. Following that model description is an explanation of the numerical methods we used to implement the model. Simulations under various settings were conducted and their results and biological interpretation are presented. Finally, we develop two new models to explore the issue of coexistence of multiple algal species under various nutrient constraints using numerical simulations.

2 One Phytoplankton Species and One Nutrient Model

The following is a model used to study vertical phytoplankton distributions by Klausmeier and Lichtman in [11]. This model incorporates intra-specific competition for light and nutrients in a poorly mixed body of water. For simplifying purposes Klausmeier and Lichtman consider a one dimensional water column where the depth is indexed by z, where $0 \leq z \leq z_b$. The surface of the water column occurs at $z = 0$ and the bottom of the water column is given by z_b. The full model consists of equations for the depth distributions of biomass density, $b(z,t)$, nutrient concentrations, $R(z,t)$, and light, $I(z,t)$.

Since light and nutrients form gradients throughout bodies of water, in order to model the change in biomass density it is necessary to know which factor is limiting phytoplankton growth. The functions $f_I(I(z,t))$ and $f_R(R(z,t))$ will be used to represent the phytoplankton growth rate when light and nutrients are limiting respectively. In general, the functions f_I and f_R need to be bounded, strictly increasing functions. Following Liebig's law of the minimum, the gross phytoplankton growth rate is given by $\min(f_I(I), f_R(R))$. Biomass loss due to grazing, respiration, and death is given by a density and depth independent constant m. Combining these, we define the net per capita growth rate at depth z by $g(z,t) = \min(f_I(I(z,t)), f_R(R(z,t))) - m$.

To complete describing the dynamics of phytoplankton populations, processes describing phytoplankton movement need to be incorporated. Phytoplankton movement is divided into two components: the first being passive movement due to turbulence in the water column and the second being the active movement. For simplicity, Klausmeier and Lichtman only consider phytoplankton species which rely on flagella to swim. Passive movement is modelled by eddy diffusion with diffusion coefficient D_b which is uniform throughout the water column. This assumption is not necessary and, in general, depth dependent diffusion is permissible. To model the active movement, we introduce a velocity function ν which is dependent on the gradient of the growth rate, $\frac{\partial g}{\partial z}$, i.e. $\nu = \nu\left(\frac{\partial g}{\partial z}\right)$. Given how phytoplankton can regulate their position depending on whether light or nutrients are limiting, the biological assumption is introduced that phytoplankton will move up if the conditions are better above than they are below, and phytoplankton will move down if the conditions are better below than they are above, and phytoplankton will not move if the conditions are worse above and below. Positive velocity is oriented upward and associated to the negative z direction. Specifically we assume $\nu(.)$ is an odd, decreasing function which approaches a value ν_{max} as $\frac{\partial g}{\partial z}$ approaches negative infinity and approaches $-\nu_{max}$ as $\frac{\partial g}{\partial z}$ approaches positive infinity.

Combining physical and biological dynamics we can describe the change in phytoplankton biomass by the partial differential equation

$$\begin{aligned}\frac{\partial b}{\partial t} &= (\min(f_I(I), f_R(R)))b - mb + D_b\frac{\partial^2 b}{\partial z^2} + \frac{\partial}{\partial z}\left[\nu\left(\frac{\partial g}{\partial z}\right)b\right] \\ &= [\text{Growth}] - [\text{Loss}] + [\text{Passive Movement}] + [\text{Active Movement}]. \qquad (2.1)\end{aligned}$$

Under the assumption that phytoplankton do not enter or leave the water column

equation (2.1) has no flux boundary conditions

$$\left[-D_b\frac{\partial b}{\partial z}-\nu\left(\frac{\partial g}{\partial z}\right)b\right]\Bigg|_{z=0}=\left[-D_b\frac{\partial b}{\partial z}-\nu\left(\frac{\partial g}{\partial z}\right)b\right]\Bigg|_{z=z_b}=0. \tag{2.2}$$

Nutrients in the water column are impacted by diffusion processes and by phytoplankton through consumption and recycling from dead phytoplankton. In [11], the nutrient under consideration is phosphorus due to its role as a limiting nutrient in aquatic ecosystems. Let D_R represent the diffusion coefficient and let ε represent the proportion of the nutrients from dead phytoplankton that is immediately recycled. Then we can describe the change in the nutrients by the partial differential equation

$$\begin{aligned}\frac{\partial R}{\partial t}&=-\frac{b}{Y}\min(f_I(I),f_R(R))+D_R\frac{\partial^2 R}{\partial z^2}+\varepsilon m\frac{b}{Y}\\&=-[\text{Uptake}]+[\text{Mixing}]+[\text{Recycling}]\end{aligned} \tag{2.3}$$

where Y is the yield of phytoplankton biomass per nutrient consumed.

It is assumed that nutrients do not leave the system from the surface but are supplied at the bottom of the water column. Nutrients in the sediment are assumed to have constant concentration denoted by R_{in} and diffuse across the sediment-water interface at a rate proportional to the concentration difference of the interface. Under these assumptions we get the boundary conditions

$$\left.\frac{\partial R}{\partial z}\right|_{z=0}=0,\ \left.\frac{\partial R}{\partial z}\right|_{z=z_b}=h(R_{in}-R(z_b)) \tag{2.4}$$

where the parameter h describes the permeability of the sediment-water interface.

Finally, light at depth z is determined using the Lambert-Beer law with phytoplankton attenuation coefficient a, background attenuation coefficient a_{bg}, and incident light I_{in}. The incident light is considered to be constant in our simulations although this assumption can easily be relaxed. Using this we have the equation for

$I(z,t)$ is given by

$$I(z,t) = I_{in} \exp\left[- \int_0^z (ab(w,t) + a_{bg})dw \right]. \tag{2.5}$$

Equations (2.1)-(2.5) constitute our first model. This is a non-local, nonlinear system of integro-partial differential equations for which theoretical analysis has been conducted. Existence of solutions for (2.1)-(2.5) is investigated in [3] while asymptotic behavior of positive solutions is studied in [4].

3 Simulation Technique

In order to simulate the model, we follow the Method of Lines approach [7]. Under this approach the spatial differential operators as well as the integral term given in equation (2.5) will be replaced by discrete approximations. This will result in a large system of ordinary differential equations of the form

$$\frac{d\mathbf{b}(t)}{dt} = \mathbf{F}(\mathbf{b}(t)),\ t \geq 0 \tag{3.1}$$

where the vector $\mathbf{b} \in \mathbb{R}^n$ contains the components $b_i(t)$ resulting from the discretization. Since (3.1) is still continuous in time the resulting system of ODEs will then be solved by numerical integration.

3.1 Spatial Discretization

To begin we define a spatial grid on the one dimensional water column $0 \leq z \leq z_b$. Let $s_0 = 0$, $s_i = \left(i - \frac{1}{2}\right)\Delta z$, and $s_{N+1} = z_b$ be the spatial grid where $\Delta z = \frac{z_b}{N}$. Here N will represent the partition of the water column and will be the resulting number of ODEs present in (3.1). To simplify notation, for $i = 1, \ldots, N$ let $b_i(t)$ denote an approximation to $b(s_i, t)$. A visual representation of the discretization adapted from

[7] is given below in Figure 3.1.

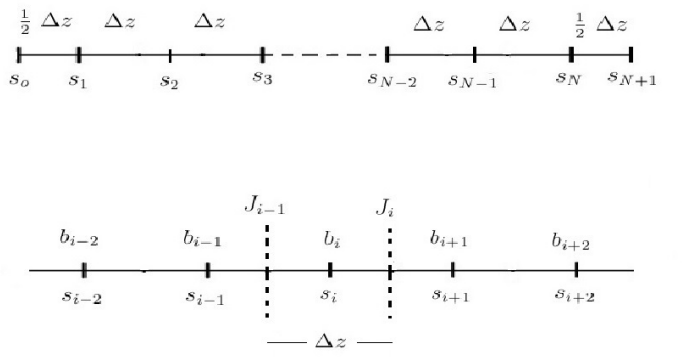

Figure 3.1: The spatial discretization of the one-dimensional water column and visual representation for discretizing the derivative of the flux.

To discretize the spatial derivatives at the points s_i present in the diffusion and active movement terms in equation (2.1) a finite volume approach is used. First define the flux of the phytoplankton by

$$J(z,t) = -\Big(\nu b(z,t) + D_b \frac{\partial b}{\partial z}(z,t)\Big). \tag{3.2}$$

The minus sign on the diffusion term is present to indicate that turbulent diffusion is in the direction opposite to the biomass concentration while the minus sign on the active movement term is a result of the orientation of the velocity.

As demonstrated in Figure 3.1, assume there is an imaginary box of size Δz around the point s_i and denote the fluxes at the side of these 'boxes' by $J_i \approx J(s_i + \frac{1}{2}\Delta z, t)$ which depends on the numerical values b_i. Doing this, conservation of J is obtained since the outflow of one part of one box will serve as the input for the adjacent box. Further, observe that equation (2.1) can be rewritten using J by

$$\frac{\partial b}{\partial t}(z,t) = g(z)b(z,t) - \frac{\partial J}{\partial z}(z,t).$$

Thus our interest is in approximating $\dfrac{\partial J}{\partial z}$ at the point $z = s_i$. To form the approximation we first split the flux into two components

$$\frac{\partial J}{\partial z}(z,t) = -\Big(\frac{\partial A}{\partial z}(z,t) - \frac{\partial P}{\partial z}(z,t)\Big) \tag{3.3}$$

where A represents the active movement portion of the flux while P represents the portion of passive movement in the flux ($D_b\dfrac{\partial b}{\partial z}$).

We use the approximation

$$\frac{\partial J}{\partial z}(z,t) \approx \frac{J_i - J_{i-1}}{\Delta z} = -\Big(\frac{A_i - A_{i-1}}{\Delta z} - \frac{P_i - P_{i-1}}{\Delta z}\Big). \tag{3.4}$$

What follows is a description of determining the approximation for J_i. For the advection term in equation (2.1) (the active movement) a third-order upwind scheme is used. The diffusion terms present in equations (2.1) and (2.3) (the passive movement) are handled using a symmetric discretization.

3.2 Biomass Advection

Under the assumptions laid out in Section 2, phytoplankton will move up or down in the water column depending on growth conditions. Thus to determine A_i under the upwinding scheme, first we need to separate the cases when $\nu_i > 0$ (upward movement) and $\nu_i < 0$ (downward movement). Further, movement near the surface of the water column and near the bottom of the water column have to be treated separately. No flux boundary conditions tell us that there cannot be upward movement at the surface or any downward motion on the bottom. However phytoplankton can swim up to the surface and down to the bottom. The surface will rely on the terms A_0, A_1, and A_2 and the bottom will rely on A_{N-2}, A_{N-1}, and A_N. The rest of the water column will rely on the terms A_i for $i = 2, \ldots, N-2$.

First consider phytoplankton that are in the water column but are not at the surface or the bottom. To implement the upwinding scheme it is necessary to know which direction the phytoplankton are swimming. When the phytoplankton are swimming down towards the bottom the flow is from left to right in Figure 3.1. For that reason more information will be used from the left. Similarly, when phytoplankton are swimming up towards the surface, the flow is from the right to the left. Separating the cases for $\nu_i > 0$ and $\nu_i < 0$ we get that the upwinding scheme in general can be given by the formula

$$\begin{aligned} A_i &= \frac{1}{6}\nu_i(2b_i + 5b_{i+1} - b_{i+2}) * (\nu_i > 0) + \frac{1}{6}\nu_i(-b_{i-1} + 5b_i + 2b_{i+1}) * (\nu_i < 0) \\ &= [\text{Upward movement}] + [\text{Downward movement}]. \end{aligned} \tag{3.5}$$

Thus the approximation to $\dfrac{\partial A}{\partial z}$ is given by

$$\begin{aligned} \frac{A_i - A_{i-1}}{\Delta z} =& \frac{1}{6\Delta z}\Big(\nu_i(2b_i + 5b_{i+1} - b_{i+2}) * (\nu_i > 0) \\ &+ \nu_i(-b_{i-1} + 5b_i + 2b_{i+1}) * (\nu_i < 0) \\ &- \nu_{i-1}(2b_{i-1} + 5b_i - b_{i+1}) * (\nu_{i-1} > 0) \\ &- \nu_{i-1}(-b_{i-2} + 5b_{i-1} + 2b_i) * (\nu_{i-1} < 0)\Big). \end{aligned}$$

Combining like terms and reorganizing we get

$$\begin{aligned} \frac{A_i - A_{i-1}}{\Delta z} =& \frac{1}{6\Delta z}\Big(\nu_{i-1} * (\nu_{i-1} < 0)b_{i-2} - (\nu_i * (\nu_i < 0) + 2\nu_{i-1} * (\nu_{i-1} > 0) \\ &- 5\nu_{i-1} * (\nu_{i-1} < 0))b_{i-1} + (2\nu_i * (\nu_i > 0) + 5\nu_i * (\nu_i < 0) \\ &- 5\nu_{i-1} * (\nu_{i-1} > 0) - 2\nu_{i-1} * (\nu_{i-1} < 0))b_i + (5\nu_i * (\nu_i > 0) \\ &+ 2\nu_i * (\nu_i < 0) + \nu_{i-1} * (\nu_{i-1} > 0))b_{i+1} - \nu_i * (\nu_i > 0)b_{i+2}\Big). \end{aligned}$$

Now consider phytoplankton near the surface of the water column. Unlike the

upwinding scheme used on A_i for $i = 2, \ldots, N-2$, the upwinding scheme for A_0 and A_1 have to be modified. Given that the system is closed we have $A_0 = 0$. To compute A_1 observe that A_1 depends only on b_1, b_2, and b_3. Using this, A_1 can be computed using the formula

$$A_1 = \nu_1 * (\nu_1 < 0)\Big(\frac{b_1 + b_2}{2}\Big) + \frac{1}{6}\nu_1 * (\nu_1 > 0)(2b_1 + 5b_2 - b_3). \tag{3.6}$$

Using the same strategy as before we construct the approximations $\dfrac{\partial A}{\partial z}$ for $z = s_1$ and $z = s_2$. For $z = s_1$ we get

$$\frac{\partial A}{\partial z}(s_1, t) \approx \frac{A_1 - A_0}{\Delta z} = \frac{1}{6\Delta z}\Big((3\nu_1 * (\nu_1 < 0) + 2\nu_1 * (\nu_1 > 0))b_1 + (3\nu_1 * (\nu_1 < 0) + 5\nu_1 * (\nu_1 > 0))b_2 - \nu_1 * (\nu_1 > 0)b_3\Big).$$

For $z = s_2$ we get

$$\frac{\partial A}{\partial z}(s_2, t) \approx \frac{A_2 - A_1}{\Delta z} = \frac{1}{6\Delta z}\Big((-\nu_2 * (\nu_2 < 0) - 3\nu_1 * (\nu_1 < 0) - 2\nu_1 * (\nu_1 > 0))b_1$$

$$+(2\nu_2 * (\nu_2 > 0) + 5\nu_2 * (\nu_1 < 0) - 5\nu_1 * (\nu_1 > 0) - 3\nu_1 * (\nu_1 < 0))b_2$$

$$+(5\nu_2 * (\nu_2 > 0) + 2\nu_2 * (\nu_2 < 0) + \nu_1 * (\nu_1 > 0))b_3 - \nu_2 * (\nu_2 > 0)b_4\Big).$$

Finally, consider phytoplankton near the bottom of the water column. As with the computations near the surface, the upwinding scheme for A_{N-1} and A_N has to be modified. As with A_0, since the system is closed it follows that $A_N = 0$. To compute A_{N-1} observe that A_{N-1} will depend on b_{N-2}, b_{N-1}, and b_N. Hence we get

$$A_{N-1} = \nu_{N-1} * (\nu_{N-1} > 0)\Big(\frac{b_N + b_{N-1}}{2}\Big) + \frac{1}{6}\nu_{N-1} * (\nu_{N-1} < 0)(-b_{N-2} + 5b_{N-1} + 2b_N). \tag{3.7}$$

Using this we finish constructing the approximations of $\dfrac{\partial A}{\partial z}$ by computing the

approximations at $z = s_{N-1}$ and $z = s_N$. At $z = s_N$ we get

$$\begin{aligned}\frac{\partial A}{\partial z}(s_N, t) \approx \frac{A_N - A_{N-1}}{\Delta z} = \frac{1}{6\Delta z}\Big(&\nu_{N-1} * (\nu_{N-1} < 0) b_{N-2} \\ &+ (-3\nu_{N-1} * (\nu_{N-1} > 0) - 5\nu_{N-1} * (\nu_{N-1} < 0)) b_{N-1} \\ &+ (-3\nu_{N-1} * (\nu_{N-1} > 0) - 2\nu_{N-1} * (\nu_{N-1} < 0)) b_N \Big).\end{aligned}$$

Finally, at $z = s_{N-1}$ we get

$$\begin{aligned}\frac{\partial A}{\partial z}(s_{N-1}, t) \approx \frac{A_{N-1} - A_{N-2}}{\Delta z} = \frac{1}{6\Delta z}\Big(&\nu_{N-2} * (\nu_{N-2} < 0) b_{N-3} \\ &+ (-\nu_{N-1} * (\nu_{N-1} < 0) - 2\nu_{N-2} * (\nu_{N-2} > 0) \\ &- 5\nu_{N-2} * (\nu_{N-2} < 0)) b_{N-2} + (5\nu_{N-1} * (\nu_{N-1} < 0) \\ &+ 3\nu_{N-1} * (\nu_{N-1} > 0) - 5\nu_{N-2} * (\nu_{N-2} > 0) \\ &- 2\nu_{N-2} * (\nu_{N-2} < 0)) b_{N-1} \\ &+ (2\nu_{N-1} * (\nu_{N-1} < 0) + \nu_{N-2} * (\nu_{N-2} > 0)) b_N \Big).\end{aligned}$$

Using these approximations, one can construct the active movement matrix, AM, such that $AM\mathbf{b}$ gives the approximations to $\dfrac{\partial A}{\partial z}$. The active movement matrix will be an $N \times N$ sparse matrix whose coefficients are given by the velocities ν_i with their corresponding positive and negative parts. This matrix will be a banded matrix which has non-zero elements in the two diagonal arrays above and the two diagonal arrays below the main diagonal, and non-zero elements in the main diagonal.

3.3 Biomass Diffusion

To finish the discretization of the biomass flux, the spatial derivatives present from the diffusion term need to be approximated. Unlike the active movement problem

where a symmetric difference can produce unwanted numerical artifacts [7], we use a symmetric method to discretize the diffusion for both the biomass and the nutrients.

Let $P_i = P(s_i + \frac{1}{2}\Delta z)$. Since the system is closed for phytoplankton at the surface and the bottom of the water column, we have $P_0 = P_N = 0$. For $i = 1, \ldots, N-1$ we have

$$P_i = D_i \frac{b_{i+1} - b_i}{\Delta z}. \tag{3.8}$$

Using (3.7) we form the approximations to the diffusion term of $\dfrac{\partial P}{\partial z}$ by computing (3.3) using the appropriate differences. Computing the differences we get

$$\frac{P_1 - P_0}{\Delta z} = \frac{1}{(\Delta z)^2}(D_1 b_1 - D_1 b_2), \tag{3.9}$$

$$\frac{P_i - P_{i-1}}{\Delta z} = \frac{1}{(\Delta z)^2}(-D_i b_{i+1} + (D_i + D_{i-1}) b_i - D_i b_{i+1}), \tag{3.10}$$

$$\frac{P_N - P_{N-1}}{\Delta z} = \frac{1}{(\Delta z)^2}(-D_{N-1} b_{N-1} + D_{N-1} b_N). \tag{3.11}$$

Thus the resulting biomass diffusion matrix, PM, will be an $N \times N$ tridiagonal matrix. The main diagonal will consist of $\dfrac{1}{(\Delta z)^2} D_1$, $\dfrac{1}{(\Delta z)^2}(D_i + D_{i-1})$, and $\dfrac{1}{(\Delta z)^2} D_{N-1}$. The upper and lower diagonals will consist of elements of the form $-\dfrac{1}{(\Delta z)^2} D_i$ where $i = 2, \ldots, N$ for the lower diagonal and $i = 1, \ldots, N-1$ for the upper diagonal.

3.4 Nutrient Diffusion

While the nutrient diffusion matrix that results from the discretization is almost identical to the biomass diffusion matrix constructed above there is a key difference. Unlike the biomass, the model developed by Klausmeier and Lichtman is not assumed to be a closed system for the nutrients. The boundary terms given in (2.4) show

that nutrients can be supplied from the sedimentary layer at the bottom of the water column. So while equations (3.8) and (3.9) will still be valid for the nutrients equation, (3.10) will no longer hold in this circumstance.

Using the boundary term for $\frac{\partial R}{\partial z}$ at $z = z_b$ we can define P_N by the equation

$$P_N = \frac{D_N}{\Delta z}\Big(h(R_{in} - R_N)\Big). \tag{3.12}$$

Proceeding as we did before, we now calculate the approximation of $\frac{\partial P}{\partial z}(z,t)$ at $z = s_N$. Using (3.7) (making the change from b_i to R_i) and (3.11) we get

$$\frac{P_N - P_{N-1}}{\Delta z} = \frac{1}{(\Delta z)^2}(-D_N h R_{in} + (D_N h + D_{N-1})R_N + -D_{N-1}R_{N-1}).$$

Note that in addition to changing the (N, N) entry, the boundary term also introduces a vector which is 0 for the first $N-1$ entries and a fixed constant for its N-th term.

4 Model Simulation

As outlined in the previous section applying the discretization to the model given by equations (2.1) - (2.5) results in a large system of ordinary differential equations. Since the resulting ODE model (3.1) is stiff, i.e., the eigenvalues of the Jacobian matrix $\frac{\partial \mathbf{F}}{\partial \mathbf{b}}$ are widely spread apart, to numerically solve the system an implicit integration method is needed. In this treatment, we implemented the model in MATLAB and integrated using MATLAB's ODE solver ode15s [1].

In order to implement the model, functional representations of $f_I(I)$, $f_R(R)$, and $\nu\Big(\frac{\partial g}{\partial z}\Big)$ are required along with the parameter values present in equations (2.1) - (2.5). Following [11], the functions f_I and f_R will have a Michaelis-Menten representation

$$f_I(I(z,t)) = r\,\frac{I(z,t)}{I(z,t) + K_I} \tag{4.1}$$

and

$$f_R(R(z,t)) = r\,\frac{R(z,t)}{R(z,t)+K_R}, \tag{4.2}$$

where K_I and K_R are the half-saturation constants for the light and nutrients respectively. Finally, following [14] the function ν used for the simulations is given by

$$\nu\Big(\frac{\partial g}{\partial z}\Big) = -\nu_{max}\,\frac{\frac{\partial g}{\partial z}}{|\frac{\partial g}{\partial z}| + K_{swim}}. \tag{4.3}$$

The parameter values used for the simulations along with their biological interpretations are reported below in Table 4.1.

Parameter	Explanation	Value	Source
N	Spatial discretization level	100	
z_b	Water column depth (m)	20	[11]
R_{in}	Sediment P concentration (μg P L^{-1})	100	[11]
h	Sediment-water column permeability (m^{-1})	10^{-2}	[11]
I_{in}	Incoming light (μmol photons m^{-2} s^{-1})	1,400	[11]
a_{bg}	Background attenuation coefficient (m^{-1})	0.35	[11], [12]
a	Algal attenuation coefficient (m^{-1} [cells ml^{-1}]$^{-1}$)	10^{-5}	[11], [12]
D_b	Eddy biomass diffusion coefficient (m^2 d^{-1})	10	[11]
D_R	Eddy nutrient diffusion coefficient (m^2 d^{-1})	10	[11]
ν_{max}	Species 1 swimming speed (m d^{-1})	10^*	[11]
r	Maximum growth rate (d^{-1})	0.4	[11]
m	Loss rate (d^{-1})	0.2	[11]
K_R	P half-saturation constant (μg P L^{-1})	1.0	[11]
K_I	Light half-saturation constant (μmol photons m^{-2} s^{-1})	50	[11]
Y	Yield coefficient (cells ml^{-1} [μg P L^{-1}]$^{-1}$)	10^3	[11]
ε	Recycling coefficient (dimensionless)	0.9^*	[14]
K_{swim}	Swimming constant (m^{-1} d^{-1})	0.001	[14]

Table 4.1: Parameters used in the simulation of the model (2.1)-(2.5). Parameter values listed with a $*$ superscript are varied to study their effect on population dynamics.

For initial conditions suppose that $b(z,0) = 10^4$ cells ml^{-1} and $R(z,0) = 1.25$ μg P L^{-1} holds for all z such that $0 \le z \le z_b$. All simulations throughout this sec-

tion are set to model the changes of the phytoplankton population density and the changes in the concentration of phosphorus for a period of time. Since our interest is investigating phytoplankton layer formation, the simulations are run until the model reaches equilibrium [11]. The simulations presented here examine the effects of the parameters ν_{max} and ε as they are varied in biologically feasible intervals. These two parameters are of interest because of their intrinsic relationship with the phytoplankton's access to nutrients in the environment. The first set of simulations examines changes in the vertical distribution as the parameter ε is increased while ν_{max} is held constant at $\nu_{max} = 10$. The second set of simulations examines the effects of reducing ν_{max} from the value given in Table 4.1 while $\varepsilon = 0$ is held constant throughout.

Given equation (2.3) it is apparent that $0 \leq \varepsilon < 1$. To examine the effects that this parameter has on the phytoplankton distribution throughout the water column three different scenarios are considered. The first case is $\varepsilon = 0$ which would imply that no nutrient content is released into the water column upon phytoplankton death. Then ε will be increased to 0.45 and then finally to 0.9 to see the effects of nutrient recycling.

As the parameter ε is increased overall phytoplankton abundance will increase. This phenomenon is occurring because increasing ε will increase the amount of free phosphorus present in the water column. While the location of the phytoplankton bloom did not change when ε was increased from 0 to 0.45, the bloom moved closer to the surface when ε was set to 0.9. This represents the surface scum layering phenomenon. Under this setting the amount of phosphorus present in the water column will not be limiting to the phytoplankton growth as can be seen in panel C.

Comparing the nutrient distributions from panels A and B to the nutrient distribution in panel C, first note the difference in scale. While panels A and B range from 0-12 μg P L^{-1}, panel C ranges from 0-18 μg P L^{-1}. Further, while the nutrient distributions in panels A and B are nearly identical, panel B has nearly double the

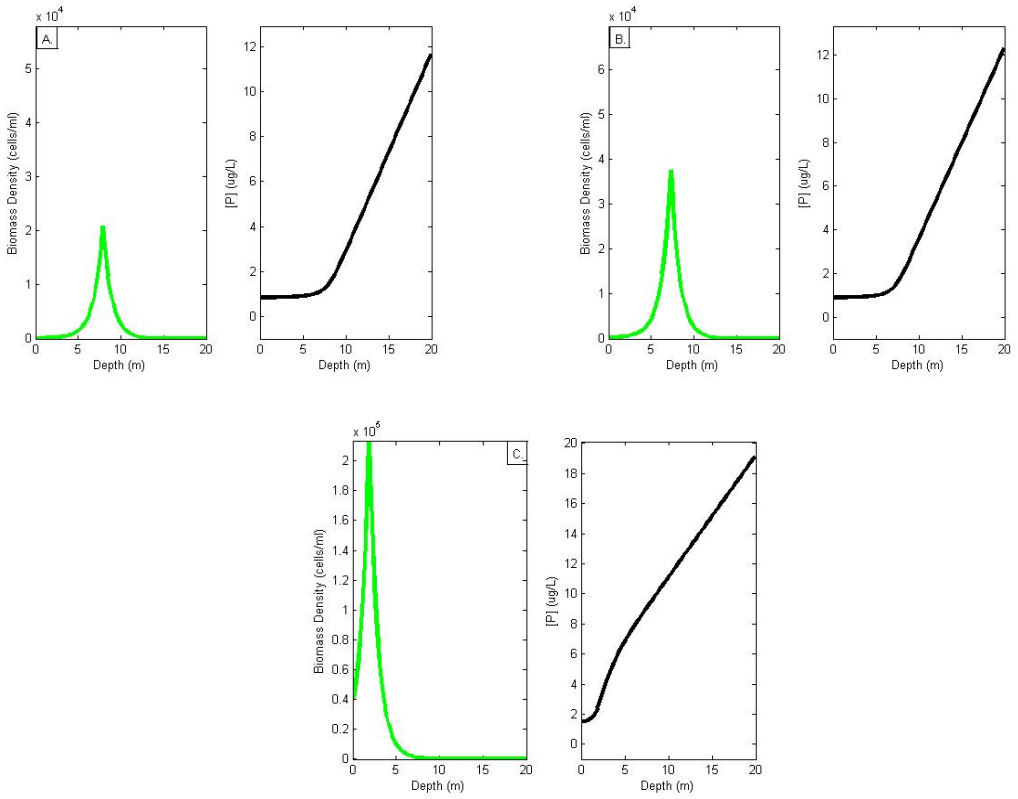

Figure 4.1: Model (2.1)-(2.5) simulations under varying levels of ε. Panel A represents the case $\varepsilon = 0$. Panel B represents the case $\varepsilon = 0.45$. Panel C represents the case $\varepsilon = 0.9$.

biomass density as panel A while the biomass in panel C has nearly an order 10 difference from panel A. In panel C, not only is there more nutrient available at the surface, the amount of nutrients available increases much more rapidly as the depth increases.

Now consider the parameter ν_{max}. Unlike ε there are no automatic constraints on what ν_{max} can be in simulations. For purposes of biological feasibility suppose, that $\nu_{max} \leq \frac{1}{2} z_b$. Since photosynthesis requires a balance between light exposure and nutrients, the speed that phytoplankton can swim in order to regulate their position in the water column is critical for growth. To study the effects that ν_{max} has on the phytoplankton density distribution we consider three cases. The first case will be $\nu_{max} = 0$, in which case the only process controlling phytoplankton movement is the

diffusion. Then the case of low versus high swimming speeds will be compared by setting $\nu_{max} = 1$ and $\nu_{max} = 10$.

As can be seen in the figure below, swimming speed has a major impact on the biomass distribution and the nutrient distribution. When $\nu_{max} = 0$ there is a major loss of biomass from the initial condition. The remaining phytoplankton are then stratified in such a way that those at the surface will automatically have the best possible growth rate because light is abundant and nutrients are supplied via diffusion. Phytoplankton not at the surface have their light reduced by shading from the biomass above. Thus as the depth increases the water column is able to support less biomass despite the abundance of nutrients. With swimming, phytoplankton near the surface move toward the bottom in order to access the nutrients deeper down in the water column while phytoplankton deep in the water column will move toward the surface to get more light. This creates the changes seen in the nutrient distributions between the simulations. These changes are due to the amount of biomass in the system. When $\nu_{max} = 0$, the biomass density is 4.202×10^4 cells ml^{-1}. With swimming, the biomass density is 4.272×10^4 cells ml^{-1} when $\nu_{max} = 1$ and 4.416×10^4 cells ml^{-1} when $\nu_{max} = 10$.

Another factor impacting the thickness of a layer is the turbulent diffusion. The width of a layer of phytoplankton swimming toward a preferred depth and mixed by turbulent diffusion is proportional to $\frac{D_b}{\nu_{max}}$. Thus, as the swimming speed increases, the thickness of the DCM's decreases when the diffusion is held constant as exhibited in Figure 4.2 panels B and C. When mixing conditions are poor, the thickness ranges between 0.1-1 m while under well mixed conditions the thickness of a layer ranges between 10-100 m [11].

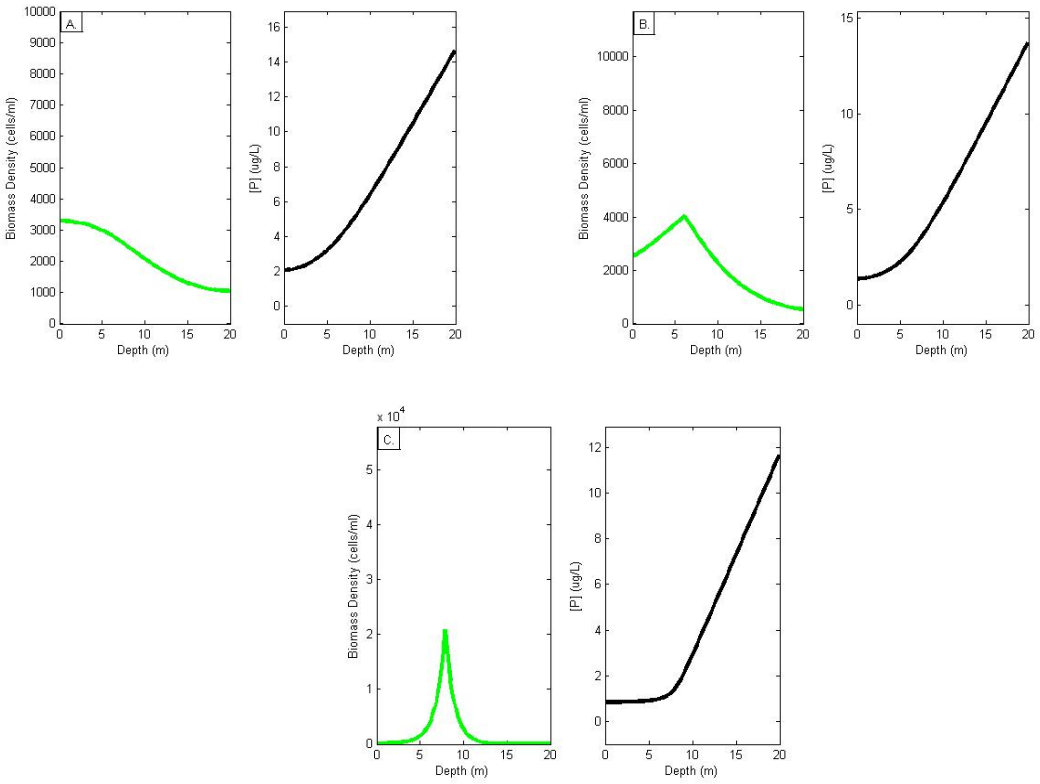

Figure 4.2: Model (2.1)-(2.5) simulations under varying levels of ν_{max}. Panel A represents the case $\nu_{max} = 0$. Panel B represents the case $\nu_{max} = 1$. Panel C represents the case $\nu_{max} = 10$.

5 Coexistence of Multiple Phytoplankton Species

While the model proposed by Klausmeier and Lichtman is able to successfully replicate common vertical phytoplankton distributions such as surface blooms and deep chlorophyll maxima, it does not provide insights into more complex ecological phenomenon. In particular, their model does not provide any explanations for why it is possible for multiple phytoplankton species to coexist in the same body of water. Biologists researching this problem have argued that the diversity of phytoplankton could be explained by using an argument involving the principle of competitive exclusion [10], [17].

The principle of competitive exclusion postulates that two or more species com-

peting for the same resources cannot coexist if other environmental factors are held constant. In this setting, one species would out-compete all the other species present so that the final equilibrium state would consist of a single species population. G.E. Hutchinson (1961) proposed that the diversity of phytoplankton could be explained phenomenologically as the failure to ever reach an equilibrium state as the environmental factors changed. Ecologically this argument is contradicted from various field observations [10], [19].

To resolve this dilemma MacArthur and Levins (1964) modify the above argument. Their idea is that phytoplankton specialize on a particular proportion of mixture of two or more resources rather than specializing on a uniform resource. In this setting, it is hypothesized that a particular species will be found where their favorite proportion is found. When the environmental factors change, then that particular species will be replaced by another species which is more effective under the new conditions [13].

In this section, two new models are developed which explore the above hypothesis. For purposes of simplicity the proposed models explore the competition of two phytoplankton species under different nutrient conditions in the environment. The first model is an extension of [11] and examines competition for one limiting nutrient. The second model investigates population dynamics when the phytoplankton species have to compete for a preferred nutrient when two limiting nutrients are present.

5.1 Two Species Competing for One Limiting Nutrient

The following is a model to study the coexistence of two phytoplankton species in a poorly mixed body of water with one limiting nutrient. The phytoplankton species are assumed to compete in uptake of the limiting nutrient and light absorption. As before, for simplifying purposes consider the one dimensional water column index by z, where $0 \leq z \leq z_b$. The full model will consist of a non-local, nonlinear system of integro-partial differential equations for the depth distributions of biomass densities

$b_1(z,t)$ and $b_2(z,t)$, the limiting nutrient concentration $R(z,t)$, and light $I(z,t)$.

Biomass densities are assumed to be limited by the availability of light and nutrients. The functions $f_{I,1}(I(z,t))$ and $f_{I,2}(I(z,t))$ will represent the phytoplankton growth rate when light is limiting for species 1 and species 2 respectively while the functions $f_{R,1}(R(z,t))$ and $f_{R,2}(R(z,t))$ will represent the phytoplankton growth rate when nutrients are limiting for species 1 and 2 respectively. The functions $f_{I,1}(I)$, $f_{I,2}(I)$, $f_{R,1}(R)$, and $f_{R,2}$ are assumed to be stricly increasing and bounded. As with the previous model, the gross phytoplankton growth rate of each species will follow the Liebig law of the minimum so that the per-capita growth rate will be given by the equations $g_k(z,t) = \min(f_{I,k}(I(z,t)), f_{R,k}(R(z,t))) - m_k$ where the index $k = 1, 2$ represents the respective species. Finally, each phytoplankton species will be effected by their movement within the water column. The movement of each species is assumed to be effected by the processes of diffusion and active movement as outlined in Section 2. The resulting partial differential equations for biomass densities are given by

$$\begin{aligned}\frac{\partial b_1}{\partial t} &= \min(f_{I,1}(I), f_{R,1}(R))b_1 - m_1 b_1 + D_{b_1}\frac{\partial^2 b_1}{\partial z^2} + \frac{\partial}{\partial z}\Big[\nu_1\Big(\frac{\partial g_1}{\partial z}\Big)b_1\Big] \\ &= [\text{Growth}] - [\text{Loss}] + [\text{Passive movement}] + [\text{Active movement}] \end{aligned} \tag{5.1}$$

and

$$\begin{aligned}\frac{\partial b_2}{\partial t} &= \min(f_{I,2}(I), f_{R,2}(R))b_2 - m_2 b_2 + D_{b_2}\frac{\partial^2 b_2}{\partial z^2} + \frac{\partial}{\partial z}\Big[\nu_2\Big(\frac{\partial g_2}{\partial z}\Big)b_2\Big] \\ &= [\text{Growth}] - [\text{Loss}] + [\text{Passive movement}] + [\text{Active movement}]. \end{aligned} \tag{5.2}$$

These partial differential equations are given no flux boundary conditions

$$\left[-D_{b_1}\frac{\partial b_1}{\partial z} - \nu_1\left(\frac{\partial g_1}{\partial z}\right)b_1\right]\Bigg|_{z=0} = \left[-D_{b_1}\frac{\partial b_1}{\partial z} - \nu_1\left(\frac{\partial g_1}{\partial z}\right)b_1\right]\Bigg|_{z=z_b} = 0, \tag{5.3}$$

and

$$\left[-D_{b_2}\frac{\partial g_2}{\partial z}-\nu_2\left(\frac{\partial g_2}{\partial z}\right)b_2\right]\Bigg|_{z=0}=\left[-D_{b_2}\frac{\partial g_2}{\partial z}-\nu_2\left(\frac{\partial g_2}{\partial z}\right)b_2\right]\Bigg|_{z=z_b}=0. \tag{5.4}$$

For the simulations, the functions $f_{I,k}$ and $f_{R,k}$ for $k=1,2$ will take the Michaelis-Menten forms given by

$$f_{I,1}(I(z,t))=r_1\,\frac{I(z,t)}{I(z,t)+K_{I,1}},$$

$$f_{I,2}(I(z,t))=r_2\,\frac{I(z,t)}{I(z,t)+K_{I,2}},$$

$$f_{R,1}(R(z,t))=r_1\,\frac{R(z,t)}{R(z,t)+K_{R,1}},$$

and

$$f_{R,2}(R(z,t))=r_2\,\frac{R(z,t)}{R(z,t)+K_{R,2}}$$

where r_1 and r_2 are the maximal growth rates of species 1 and 2 respectively and the $K_{I,1}$, $K_{I,2}$, $K_{R,1}$, and $K_{R,2}$ represent half-saturation constants for light and nutrients for species 1 and 2 respectively. Following equation (4.3) the functions ν_1 and ν_2 will take the form

$$\nu_1\Big(\frac{\partial g_1}{\partial z}\Big)=-\nu_{1_{max}}\,\frac{\frac{\partial g_1}{\partial z}}{|\frac{\partial g_1}{\partial z}|+K_{swim}}$$

and

$$\nu_2\Big(\frac{\partial g_2}{\partial z}\Big)=-\nu_{2_{max}}\,\frac{\frac{\partial g_2}{\partial z}}{|\frac{\partial g_2}{\partial z}|+K_{swim}}.$$

As before, nutrients in the water column are impacted by diffusion processes and by phytoplankton from consumption and recycling. Let D_R represent the diffusion coefficient of the nutrients and let ε represent the proportion of nutrients that are available in the water column from dead phytoplankton. The change in the limiting

nutrient R is given by the partial differential equation

$$\begin{aligned}\frac{\partial R}{\partial t} &= -\frac{b_1}{Y_1}\min(f_{I,1}(I), f_{R,1}(R)) + \varepsilon\,\frac{b_1}{Y_1} - \frac{b_2}{Y_2}\min(f_{I,2}(I), f_{R,2}(R)) \\ &\quad + \varepsilon\,\frac{b_2}{Y_2} + D_R\,\frac{\partial^2 R}{\partial z^2} \\ &= -[\text{Species 1 Uptake}] + [\text{Species 1 Recycling}] - [\text{Species 2 Uptake}] \\ &\quad + [\text{Species 2 Recycling}] + [\text{Mixing}]. \end{aligned} \tag{5.5}$$

Nutrients are not assumed to enter or leave the water column from the surface but are supplied from the sedimentary layer at the bottom. Thus we have the boundary conditions for equation (5.5) will be given by equation (2.4).

Finally, to describe the change in light at depth z, we modify the Lambert-Beer law to accommodate the presence of multiple phytoplankton species. Assuming that the relationship between the number of species present and the light absorption is linear, equation (2.5) is modified to become

$$I(z,t) = I_{in}\exp\left[-\int_0^z (ab_1(w,t) + ab_2(w,t) + a_{bg})dw\right] \tag{5.6}$$

where the parameters I_{in}, a, and a_{bg} have the same interpretation as before. Equations (5.1)-(5.6) constitute our model.

Parameter interpretation and values used for the simulations can be found in Table 5.1. To test the assertion that MacArthur and Levins made, the parameters that need to be different than those given in [11] and [14] are $K_{I,2}$, $K_{R,2}$, and m_2. The half-saturation constants for light and nutrients used in the growth rate affect the proportion of light and nutrients needed by a species. For this reason, these parameters are chosen such that $K_{I,2} < K_{I,1}$ and $K_{R,2} > K_{R,1}$. This way the competing species will have growth rates defined in such a way that the first species has a growth rate with proportionally larger requirement on light while the second species has a

growth rate with proportionally larger nutrient requirements. With these assumptions, the phytoplankton species will have natural niches located at different depths that they will want to occupy. Finally, in order to test the hypothesis that MacArthur and Levins made, the phytoplankton species will need to have different loss rates. If $m_1 = m_2$ then the principle of competitive exclusion would hold and the model would give the extinction of one of the phytoplankton species.

For initial conditions suppose that $b_1(z,0) = b_2(z,0) = 10^4$ cells ml^{-1} and $R(z,0) = 1.25$ μg P L^{-1} holds for all z such that $0 \leq z \leq z_b$. As in Section 4, the simulations throughout this section are set to model the changes of the phytoplankton population density and the changes in the concentration of phosphorus over a period of time to investigate the layer formation patterns that the two species model exhibits. Like with our first model, the simulations presented here examine the effects of the parameters $\nu_{1_{max}}$, $\nu_{2_{max}}$ and ε as they are varied in biologically feasible intervals.

As in Section 4, the three values of ε used to study the impact of nutrient recycling are $\varepsilon = 0$, 0.45, and 0.9 while the swimming speeds are kept constant at $\nu_{1_{max}} = \nu_{2_{max}} = 10$. The vertical distributions of the two phytoplankton species and the nutrient concentration are given below in Figure 5.1.

The proposed two species model is able to replicate vertical distributions such as surface blooms (Figure 5.1 C) and the DCM (Figure 5.1 A and B). As with the model proposed by Klausmeier and Lichtman, when ε increases, the location of each species bloom moves closer to the surface and the biomass densities of both species increases. However, unlike the single species model, more ecological complexity is described. In particular Figure 5.1 implies the existence of multiple DCM's within an environment. Moreover, Figures 5.1 A and B show that the DCM's of each species are located at different depths and are non-overlapping as hypothesized by MacArthur and Levins while Figure 5.1 C demonstrates that multiple phytoplankton species are able to occupy the same layer in the water column. This heterogeneity is a key feature

Parameter	Explanation	Value	Source
N	Spatial discretization level	100	
z_b	Water column depth (m)	20	[11]
R_{in}	Sediment P concentration (μg P L^{-1})	100	[11]
h	Sediment-water column permeability (m^{-1})	10^{-2}	[11]
I_{in}	Incoming light (μmol photons m^{-2} s^{-1})	1,400	[11]
a_{bg}	Background attenuation coefficient (m^{-1})	0.35	[11], [12]
a	Algal attenuation coefficient (m^{-1} [cells $ml^{-1}]^{-1}$)	10^{-5}	[11], [12]
D_{b_1}	Species 1 biomass diffusion coefficients (m^2 d^{-1})	10	[11]
D_{b_2}	Species 2 biomass diffusion coefficients (m^2 d^{-1})	10	[11]
D_R	Nutrient diffusion coefficient (m^2 d^{-1})	10	[11]
$\nu_{1_{max}}$	Species 1 swimming speed (m d^{-1})	10^*	[11]
$\nu_{2_{max}}$	Species 2 swimming speed (m d^{-1})	10^*	[11]
r_1	Species 1 maximum growth rates (d^{-1})	0.4	[11]
r_2	Species 2 maximum growth rates (d^{-1})	0.4	[11]
m_1	Species 1 Loss rate (d^{-1})	0.2	[11]
m_2	Species 2 Loss rate (d^{-1})	0.1	
$K_{R,1}$	P half-saturation constant (μg P L^{-1})	1	[11]
$K_{R,2}$	P half-saturation constant (μg P L^{-1})	10	
$K_{I,1}$	Light half-saturation constant (μmol photons m^{-2} s^{-1})	50	[11]
$K_{I,2}$	Light half-saturation constant (μmol photons m^{-2} s^{-1})	5	
Y_1	Species 1 yield coefficient (cells ml^{-1} [μg P $L^{-1}]^{-1}$)	10^3	[11]
Y_2	Species 2 yield coefficient (cells ml^{-1} [μg P $L^{-1}]^{-1}$)	10^3	[11]
ε	Recycling coefficient (dimensionless)	0.9^*	[14]
K_{swim}	Swimming constant (m^{-1} d^{-1})	0.001	[14]

Table 5.1: Parameters used in the simulation of the model (5.1)-(5.6). Parameter values listed with a $*$ superscript are varied to study their effect on population dynamics.

of phytoplankton ecology.

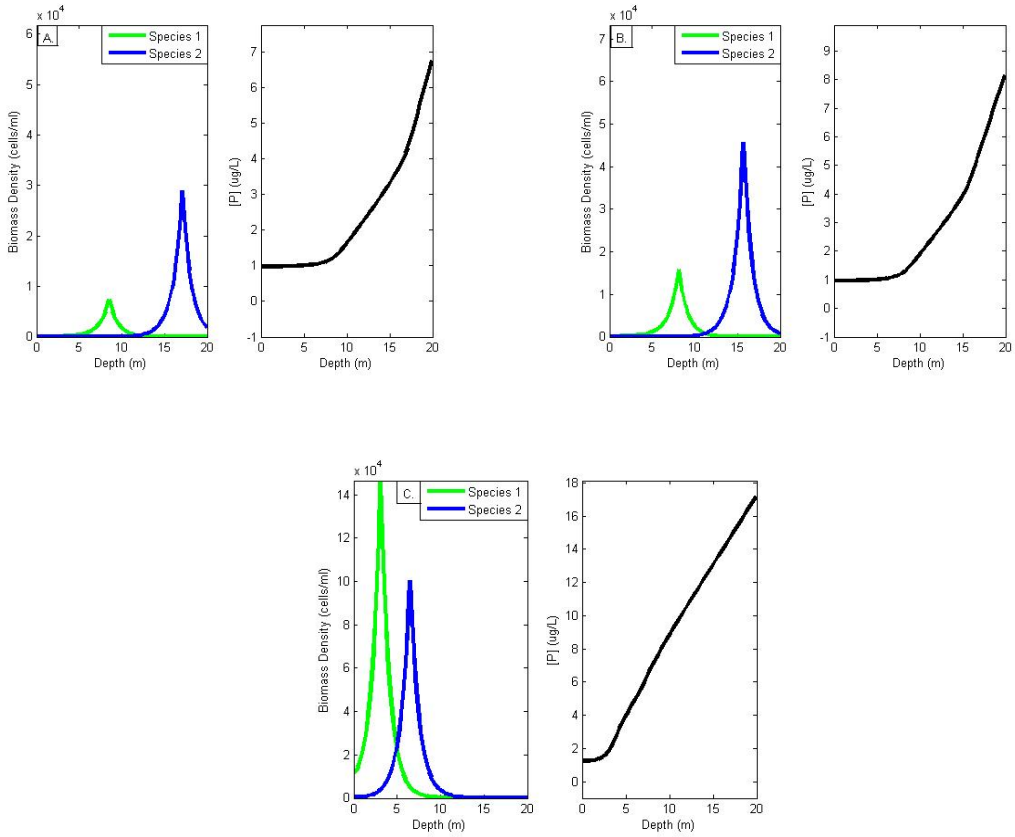

Figure 5.1: Model (5.1)-(5.6) simulations under varying levels of ε. Panel A represents the case $\varepsilon = 0$. Panel B represents the case $\varepsilon = 0.45$. Panel C represents the case $\varepsilon = 0.9$.

Now consider the parameters $\nu_{1_{max}}$ and $\nu_{2_{max}}$. In general, the model does permit these parameters having distinct values, but for purposes of this analysis assume $\nu_{1_{max}} = \nu_{2_{max}}$. The use of different swimming speeds can force the model to exhibit predictions that would be expected under the principle of competitive exclusion. For example, under the parametrization $\nu_{1_{max}} = 10$ m d^{-1}, $\nu_{2_{max}} = 1$ m d^{-1}, and $\varepsilon = 0.9$, the model predicts that species 2 would go extinct which is what we would expect given the competitive advantage species 1 has in this scenario. Since our interest is in examining what factors can explain coexistence of phytoplankton species these cases are considered pathological.

As in Section 4, for purposes of biological feasibility suppose that $\nu_{1_{max}} \leq \frac{1}{2} z_b$. For

the simulations, $\nu_{1_{max}}$ will be set to 0 m d^{-1} (diffusion only), 1 m d^{-1} (low swimming speed), and 10 m d^{-1} (high swimming speed) with $\varepsilon = 0$. As can be seen in Figure 5.2 below, the swimming speed of the phytoplankton has a major impact on the depth profiles for biomass and the nutrient gradient.

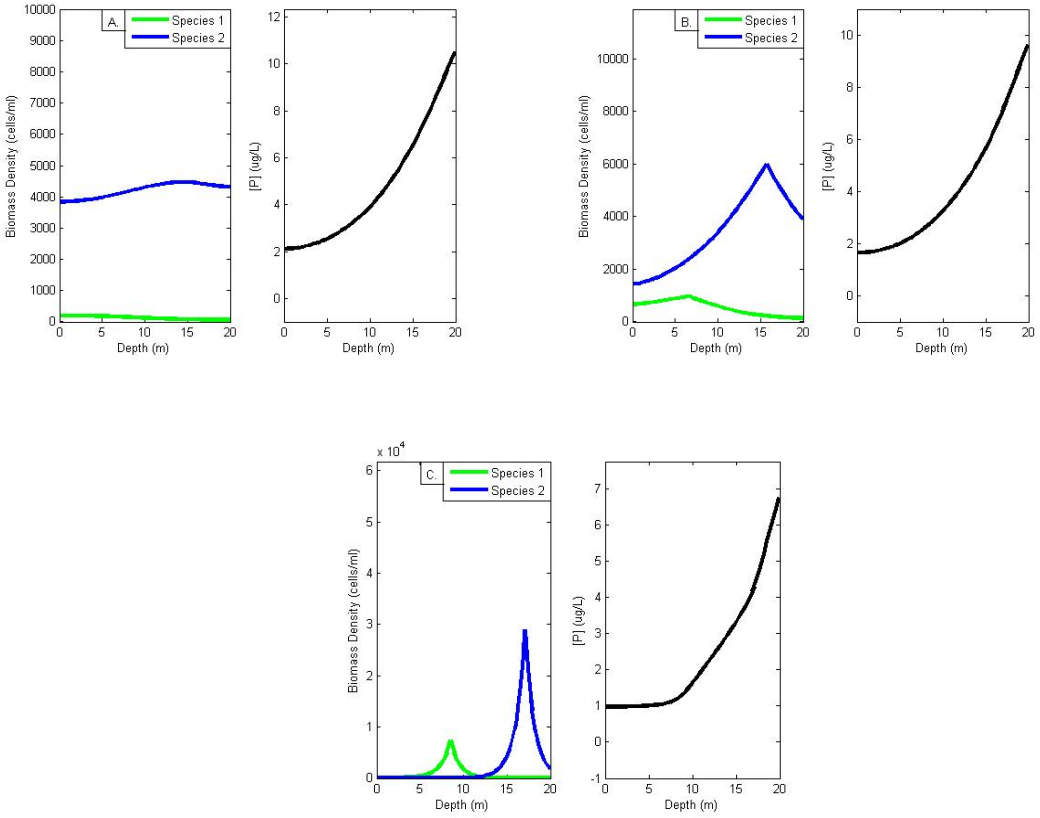

Figure 5.2: Model (5.1)-(5.6) simulations under varying levels of $\nu_{1_{max}} = \nu_{2_{max}}$. Panel A represents the case $\nu_{1_{max}} = 0$. Panel B represents the case $\nu_{1_{max}} = 1$. Panel C represents the case $\nu_{1_{max}} = 10$.

Under the setting where there is no active movement present for either species, there is a major decrease in population density from the intial conditions. However, the effect of this is more noticeable in species 1 than species 2. The reason this occurs is that the two species have different mortality rates. Without active movement, phytoplankton are only able to change position in the water column by the passive process of diffusion. While the principle of competitive exclusion would predict that species 2 would have an advantage due to its lower loss rate, as can been seen in

Figure 5.2 A, species 1 does not go completely extinct. Species 1 does not go extinct because it is designed with a growth rate that proportionally favors light to nutrients.

While Figure 5.1 A is consistent with the biological theory, Figure 5.1 B offers the most interesting ecological insights out of the three simulations. Not only are there distinct peaks in biomass densities present in different depths of the water column, neither species is absent from any depth either. Indeed, as noted above, when $\nu_{1_{max}} = \nu_{2_{max}} = 10$ m d^{-1} and $\varepsilon = 0$, the model shows that the phytoplankton stratify themselves in thin layers at their preferred niche in an independent fashion. What this suggests is that to have a heterogeneous environment throughout the water column, nutrient cycling should be present and phytoplankton swimming speed should be moderate.

To test this claim, let $\nu_{1_{max}} = 7$ m d^{-1}, $\nu_{2_{max}} = 6$ m d^{-1}, and $\varepsilon = 0.75$ and suppose that all other parameters are as reported in Table 5.1. Further, suppose that the same initial conditions hold. Figure 5.3 shows the resulting depth profiles simulated by the model.

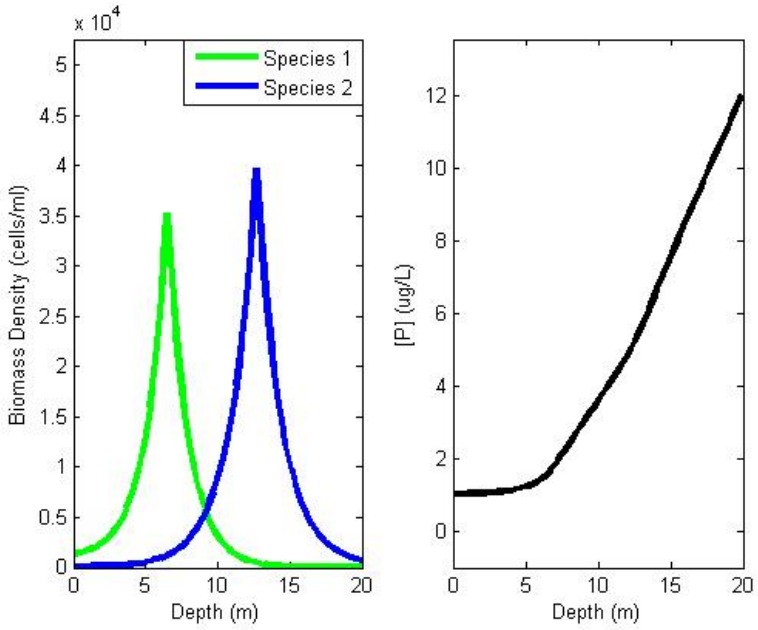

Figure 5.3: Model (5.1)-(5.6) simulation with $\nu_{1_{max}} = 7$, $\nu_{2_{max}} = 6$, and $\varepsilon = 0.75$

As hypothesized, the model under this parametrization gives a vertically heterogeneous water column. At the surface species 1 is present at approximately 1,400 cells ml^{-1} and species 2 is present at approximately 140 cells ml^{-1} while at the bottom of the water column species 1 is scarce at approximately 20 cells ml^{-1} and species 2 is present at approximately 780 cells ml^{-1}. Further, the proportional light to nutrient depth dependent niches are clearly exhibited at approximately 6.5 m deep for species 1 and at approximately 12.7 m deep for species 2. While these depths represent distinct DCM's, both phytoplankton species are shown to be able to coexist and are present in equal amounts at approximately 9.17 m. Further, the phosphorus concentration gradient is consistent with figures reported in the simulations done in [11] and [14].

5.2 Two Species With Preferential Nutrient Uptake

For the final model under consideration we modify the model given by equations (5.1)-(5.6). In all of the previous models discussed, there has been only one nutrient present in the system and it is assumed to be limiting growth. The phytoplankton were assumed to use the nutrient present to facilitate their growth. This is an idealized situation and the interaction between phytoplankton species and nutrients present in the environment are complex [16]. For example, the species *Mycrocistis* prefers to acquire nitrogen from ammonia rather than nitrate [2]. The proposed model studies the coexistence of two phytoplankton species in an environment where there are two limiting nutrients present with the assumption that one nutrient is preferentially taken up. Without loss of generality, it is assumed that R_1 is the preferred nutrient. The full model will consist of a non-local, nonlinear system of integro-partial differential equations for the depth distributions of biomass densities $b_1(z,t)$ and $b_2(z,t)$, the limiting nutrient concentrations $R_1(z,t)$ and $R_2(z,t)$, and light $I(z,t)$.

Since the phytoplankton species now have two nutrients that are drawn from

the environment, modifications to the growth terms in equations (5.1) and (5.2) need to be considered. This is done by modifying the per-capita growth rate $g_k(z)$ for species $k = 1, 2$. While we still assume that the growth of the phytoplankton species follows Liebig's law of the minimum, the functions $f_{R,1}$ and $f_{R,2}$ are now dependent on both $R_1(z,t)$ and $R_2(z,t)$. Thus the per-capita growth becomes $g_k(z,t) = \min(f_{I,k}(I(z,t), f_{R,k}(R_1(z,t), R_2(z,t)))) - m_k$ for species $k = 1, 2$ respectively. The functions $f_{R,1}(R_1, R_2)$ and $f_{R,2}(R_1, R_2)$ will take the form of a modified Michaelis-Menten equation given by

$$f_{R,1}(R_1(z,t), R_2(z,t)) = r_1 \left(\frac{R_1(z,t)}{K_{R_1,1} + R_1(z,t)} + \frac{R_2(z,t)}{K_{R_2,1} + R_2(z,t)} \, e^{-\lambda R_1(z,t)} \right) \quad (5.7)$$

and

$$f_{R,2}(R_1(z,t), R_2(z,t)) = r_2 \left(\frac{R_1(z,t)}{K_{R_1,2} + R_1(z,t)} + \frac{R_2(z,t)}{K_{R_2,2} + R_2(z,t)} \, e^{-\lambda R_1(z,t)} \right) \quad (5.8)$$

where the parameters $K_{R_1,1}$ and $K_{R_2,1}$ represent the half-saturation constants for species 1 with the corresponding nutrient, the parameters $K_{R_1,2}$ and $K_{R_2,2}$ represent the half-saturation constants for species 2 with the corresponding nutrient, and λ is an inhibition coefficient. The functions $f_{I,1}$, $f_{I,2}$, $\nu_1\left(\frac{\partial g_1}{\partial z}\right)$ and $\nu_2\left(\frac{\partial g_2}{\partial z}\right)$ will take the forms described in the previous section. Using the physical and biological assumptions established in Section 2, the equations for the biomass distributions are given by the partial differential equations

$$\begin{aligned} \frac{\partial b_1}{\partial t} &= \min(f_{I,1}(I), f_{R,1}(R_1, R_2))b_1 - m_1 b_1 + D_{b_1} \frac{\partial^2 b_1}{\partial z^2} + \frac{\partial}{\partial z}\Big[\nu_1\Big(\frac{\partial g_1}{\partial z}\Big) b_1\Big] \\ &= [\text{Growth}] - [\text{Loss}] + [\text{Passive movement}] + [\text{Active movement}] \end{aligned} \quad (5.9)$$

and

$$\begin{aligned}\frac{\partial b_2}{\partial t} &= \min(f_{I,2}(I), f_{R,2}(R_1, R_2))b_2 - m_2 b_2 + D_{b_2}\frac{\partial^2 b_2}{\partial z^2} + \frac{\partial}{\partial z}\Big[\nu_2\Big(\frac{\partial g_2}{\partial z}\Big)b_2\Big] \\ &= [\text{Growth}] - [\text{Loss}] + [\text{Passive movement}] + [\text{Active movement}]. \end{aligned} \tag{5.10}$$

These PDEs will be given no flux boundary conditions given by equations (5.3) and (5.4).

To model the change in the nutrients R_1 and R_2, modifications to nutrient uptake formulation are made. Since both species will be using both nutrients to grow, it's necessary to determine the proportion of each nutrient lost to uptake processes. Define the functions g and h by

$$g(R_k) = \frac{R_k}{K_{R_k,1} + R_k} \tag{5.11}$$

and

$$h_k(R_1, R_2) = \frac{R_2}{K_{R_2,k} + R_2}\, e^{-\lambda R_1} \tag{5.12}$$

for $k = 1, 2$. These functions will be used to give the appropriate proportion of each nutrient drawn by each species. Using these modification and the physical and biological assumptions the partial differential equations for the nutrients are given by

$$\begin{aligned}\frac{\partial R_1}{\partial t} =& -\frac{r_1}{Y_1}\min(f_{I,1}(I), f_{R,1}(R_1, R_2))\,\frac{g(R_1)}{f_{R,1}(R_1, R_2)}\,b_1 + \varepsilon m_1\,\frac{b_1}{Y_1} \\ & -\frac{r_2}{Y_2}\min(f_{I,2}(I), f_{R,2}(R_1, R_2))\,\frac{g(R_2)}{f_{R,2}(R_1, R_2)}\,b_2 + \varepsilon m_2\,\frac{b_2}{Y_2} \\ & + D_{R_1}\frac{\partial^2 R_1}{\partial z^2} \\ =& -[\text{Species 1 Uptake}] + [\text{Species 1 Recycling}] - [\text{Species 2 Uptake}] \\ & + [\text{Species 2 Recycling}] + [\text{Mixing}] \end{aligned} \tag{5.13}$$

and

$$\begin{aligned}\frac{\partial R_2}{\partial t} =& -\frac{r_1}{Y_1}\min(f_{I,1}(I), f_{R,1}(R_1,R_2))\,\frac{h_1(R_1,R_2)}{f_{R,1}(R_1,R_2)}\,b_1 + \varepsilon m_1\,\frac{b_1}{Y_1}\\ &-\frac{r_2}{Y_2}\min(f_{I,2}(I), f_{R,2}(R_1,R_2))\,\frac{h_2(R_1,R_2)}{f_{R,2}(R_1,R_2)}\,b_2 + \varepsilon m_2\,\frac{b_2}{Y_2}\\ &+ D_{R_1}\frac{\partial^2 R_1}{\partial z^2}\\ &= -[\text{Species 1 Uptake}] + [\text{Species 1 Recycling}] - [\text{Species 2 Uptake}]\\ &+ [\text{Species 2 Recycling}] + [\text{Mixing}].\end{aligned} \tag{5.14}$$

For boundary conditions on the nutrient equations, assume as in Section 2 that nutrients cannot enter or leave the water column from the surface and that both nutrients are supplied from the bottom. As before, nutrients in the sediment are assumed to have constant concentration. Let the concentration of nutrient 1 in the sediment be denoted by R_{in_1} and let the concentration of nutrient 2 in the sediment be denoted by R_{in_2}. Then we have the boundary conditions for equations (5.13) and (5.14) are given by

$$\left.\frac{\partial R_1}{\partial z}\right|_{z=0} = 0,\ \left.\frac{\partial R_1}{\partial z}\right|_{z=z_b} = h(R_{in_1} - R_1(z_b)) \tag{5.15}$$

and

$$\left.\frac{\partial R_2}{\partial z}\right|_{z=0} = 0,\ \left.\frac{\partial R_2}{\partial z}\right|_{z=z_b} = h(R_{in_2} - R_2(z_b)) \tag{5.16}$$

where h represents the permeability of the sediment-water interface.

These PDEs along with equation (5.6) form our model. Table 5.2 lists the parameter interpretations and values used in the model simulations. For initial conditions suppose $b_1(z,0) = b_2(z,0) = 10^4$ cells ml^{-1}, $R_1(z,0) = 2.25$ μg L^{-1}, and $R_2(z,0) = 2.1$

μg L^{-1} holds for all z such that $0 \leq z \leq z_b$. To investigate the phytoplankton layering patterns, model simulations are run for a time period long enough for numerical changes in phytoplankton and nutrient distributions to approximately stabilize. As before, the investigation of layer formation will focus on studying the effects of the parameters ε, $\nu_{1_{max}}$, and $\nu_{2_{max}}$. For simplifying purposes we consider situations when $\nu_{max_1} = \nu_{max_2}$ although this assumption can be relaxed.

To investigate the impact that nutrient recycling has in this model three levels of recycling are used. The first case considered, $\varepsilon = 0$, corresponds to no nutrients being released into the environment upon phytoplankton death. The cases $\varepsilon = 0.45$ and $\varepsilon = 0.9$ serve to study the impact of nutrient recycling on layer formation. For the simulations the swimming speeds of the phytoplankton are set to $\nu_{1_{max}} = \nu_{2_{max}}$ = 10 m d^{-1}. The model simulations are depicted below in Figure 5.4.

As with the previous models, panels A and B represent the formation of DCM's while panel C represents a surface scum formation. In that simulation, there is a distinct difference in the nutrient distributions compared to the distributions in Panels A and B in Figure 5.4. Not only does panel C predict that there are more nutrients present in the water column, but at the substrate the preferred nutrient for growth (Nutrient 1) is present in higher amounts than Nutrient 2. This occurs because in that simulation there is no biomass at the substrate level and since $R_{in_1} > Rin_2$ there is more supply of Nutrient 1 than Nutrient 2. Another feature of panel C which separates it from the other simulations is the support of biomass at the surface despite the fact that both nutrients are limiting at depths up to 5 m. This characteristic implies that surface scums are able to sustain their biomass by nutrient recycling under poor mixing conditions. In general, nutrient cycling helps biomass abundance of phytoplankton species. As with the previous interspecies model, Panels A and B have nearly identical nutrient distributions yet in panel B more biomass is supported by the environment. While the relative location of the DCM's has not changed

Parameter	Explanation	Value	Source
N	Spatial discretization level	100	
z_b	Water column depth (m)	20	[11]
R_{in_1}	Sediment concentration Nutrient 1 (μg L^{-1})	150	
$R)in_2$	Sediment concentration Nutrient 2 (μg L^{-1})	100	[11]
h	Sediment-water column permeability (m^{-1})	10^{-2}	[11]
I_{in}	Incoming light (μmol photons m^{-2} s^{-1})	1,400	[11]
a_{bg}	Background attenuation coefficient (m^{-1})	0.35	[11], [12]
a	Algal attenuation coefficient (m^{-1} [cells $ml^{-1}]^{-1}$)	10^{-5}	[11], [12]
D_{b_1}	Species 1 biomass diffusion coefficients (m^2 d^{-1})	10	[11]
D_{b_2}	Species 2 biomass diffusion coefficients (m^2 d^{-1})	10	[11]
D_{R_1}	Nutrient 1 diffusion coefficient (m^2 d^{-1})	10	[11]
D_{R_2}	Nutrient 2 diffusion coefficient (m^2 d^{-1})	10	[11]
$\nu_{1_{max}}$	Species 1 swimming speed (m d^{-1})	10^*	[11]
$\nu_{2_{max}}$	Species 2 swimming speed (m d^{-1})	10^*	[11]
r_1	Species 1 maximum growth rates (d^{-1})	0.4	[11]
r_2	Species 2 maximum growth rates (d^{-1})	0.4	[11]
m_1	Species 1 Loss rate (d^{-1})	0.2	[11]
m_2	Species 2 Loss rate (d^{-1})	0.1	
$K_{R_1,1}$	Nutrient 1 half-saturation constant for Species 1 (μg L^{-1})	1	[11]
$K_{R_1,2}$	Nutrient 1 half-saturation constant for Species 2 (μg L^{-1})	1	[11]
$K_{R_2,1}$	Nutrient 2 half-saturation constant for Species 1 (μg L^{-1})	10	
$K_{R_2,2}$	Nutrient 2 half-saturation constant for Species 2 (μg L^{-1})	10	
$K_{I,1}$	Light half-saturation constant (μmol photons m^{-2} s^{-1})	50	[11]
$K_{I,2}$	Light half-saturation constant (μmol photons m^{-2} s^{-1})	5	
Y_1	Species 1 yield coefficient (cells ml^{-1} [μg P $L^{-1}]^{-1}$)	10^3	[11]
Y_2	Species 2 yield coefficient (cells ml^{-1} [μg P $L^{-1}]^{-1}$)	10^3	[11]
ε	Recycling coefficient (dimensionless)	0.9^*	[14]
K_{swim}	Swimming constant (m^{-1} d^{-1})	0.001	[14]
λ	Nutrient uptake inhibition factor (dimensionless)	1	

Table 5.2: Parameters used in the simulation of the model given by equations (5.9), (5.10), (5.13), (5.14), and (5.6) . Parameter values listed with a $*$ superscript are varied to study their effect on population dynamics.

significantly, the relative abundance of species 1 nearly doubles between the two simulations.

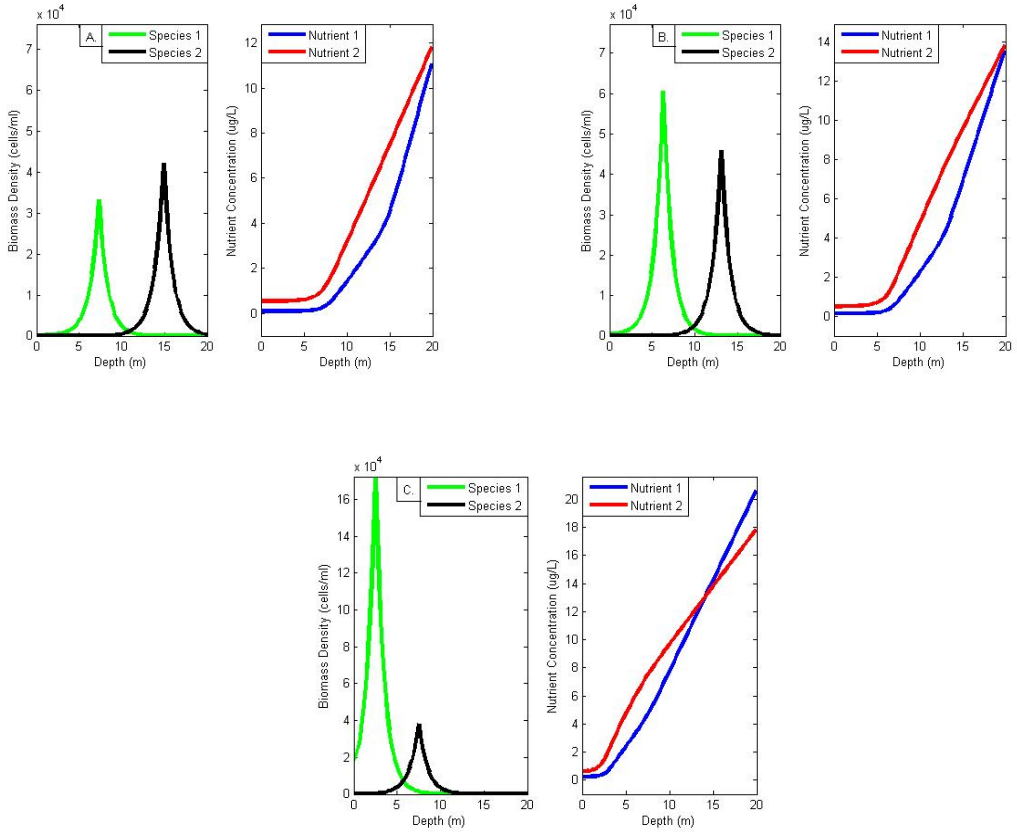

Figure 5.4: Equations (5.9), (5.10), (5.13), and (5.14) simulations under varying levels of ε. Panel A represents the case $\varepsilon = 0$. Panel B represents the case $\varepsilon = 0.45$. Panel C represents the case $\varepsilon = 0.9$.

As suggested in [11], swimming speed and levels of mixing impact the thickness of the layers that phytoplankton grow in. The previous model simulations suggest that as swimming speed $\nu_{1_{max}}$ and $\nu_{2_{max}}$ increase, the biomass layer is thinner. We test to see if this phenomenon holds in this model. Proceeding as before, we consider three different swimming speeds: $\nu_{1_{max}} = 0$ (diffusion only), $\nu_{1_{max}} = 1$ (low swimming speed), and $\nu_{1_{max}} = 10$ (high swimming speed). For these simulations we assume $\varepsilon = 0$. The results of these simulations are depicted below in Figure 5.5.

Unlike the previous multi-species model, when the phytoplankton movement is assumed to only be governed by diffusive processes, both species are present. While

the second species' biomass distribution is only affected by a drop in overall abundance (approximately 1,000 cells ml^{-1} uniformly over depth) between the previous model and the current model under consideration, species 1 biomass distribution is distinctly different. This difference is occurring because unlike the previous model, the preferred limiting nutrient concentration is approximately 0.214 μg L^{-1} at the surface (in the previous model nutrient concentrations at the surface are approximately 2 μg L^{-1}). While Nutrient 2 is present at 2.75 μg L^{-1} at the surface, it's impact on growth isn't as beneficial and since species 2 is assumed to have a growth rate which proportionally favors nutrients to light, growth is inhibited. Conversely, since species 1 is assumed to have a growth rate which proportionally favors light to nutrients, it is more abundant at the surface than in the previous model simulations.

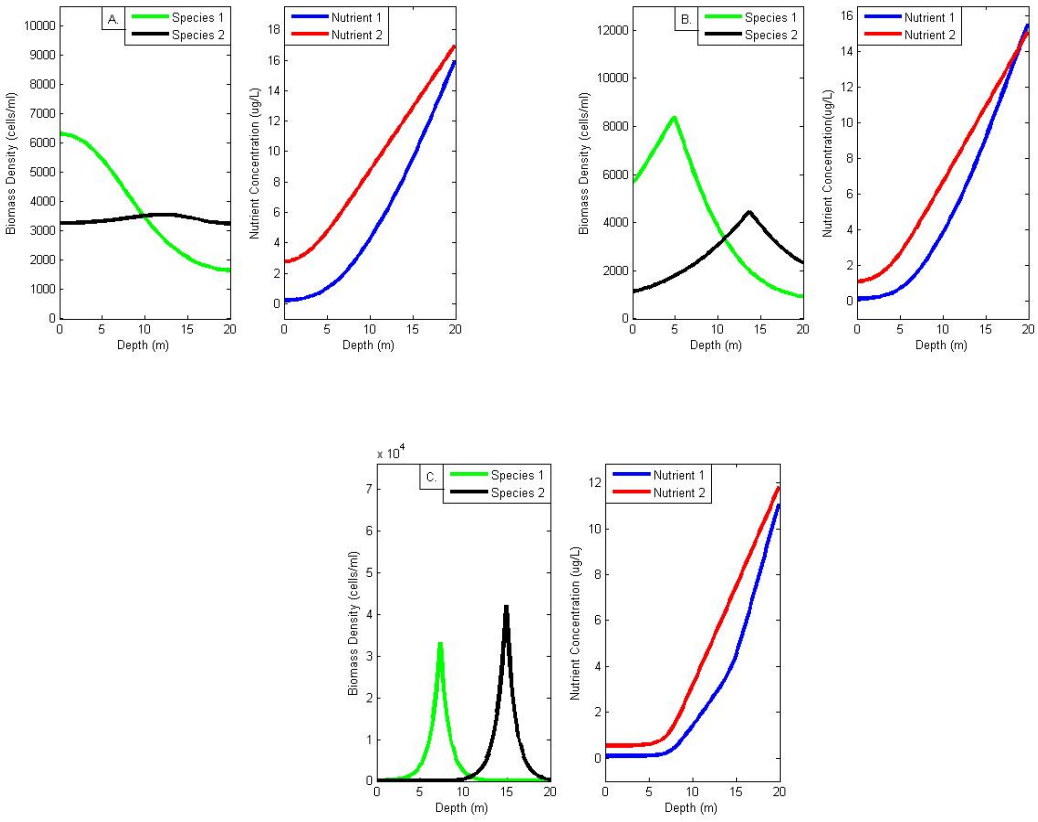

Figure 5.5: Equations (5.9), (5.10), (5.13), and (5.14) simulations under varying levels of $\nu_{1_{max}} = \nu_{2_{max}}$. Panel A represents the case $\nu_{1_{max}} = 0$. Panel B represents the case $\nu_{1_{max}} = 1$. Panel C represents the case $\nu_{1_{max}} = 10$.

While Figure 5.2 panel A differs significantly from Figure 5.5 panel A, the biomass distributions for panels B and C are similar thematically. For instance, when swimming speed is low, both species are able to coexist throughout the entire water column and two DCM's form. Furthermore, as the swimming speed increases the thickness of the DCM's decreases and the phytoplankton stratify throughout the depth at their preferred niches.

6 Conclusion and Suggestions for Future Work

The proposed multi-species models successfully replicates common layering phenomenon such as surface scums and deep chlorophyll maxima as seen in nature and in previous mathematical models such as [11] and [14]. The presence of light and nutrient gradients are essential in controlling biomass abundance and the coexistence of phytoplankton species can be attributed to how different species specialize on the proportions of light and nutrients needed to conduct photosynthesis as proposed by MacArthur and Levins. Additionally, the results from the proposed multi-species models presented here offer several avenues of continued modelling efforts.

In addition to replicating the various phenomena, the proposed multi-species models also offer insights into the relationship between a biomass layer and the ratio of phytoplankton swimming speed and the turbulence of the water. This study focused on poorly mixed bodies of water. A natural extension of our work would be to consider working with stratified water columns with various levels of mixing depending on the depth [14]. Currently we are able to show the formations of thin layers under fast swimming speeds and poor mixing. To further validate the models under consideration it would be important to study the predicted thickness of biomass layers in different environments.

Besides investigating biomass layering phenomenon in various environments to show further generality, there are theoretical avenues that our current model simu-

lations suggest could be fruitful to explore. Since the current models do predict the formation of thin layers as swimming speed is increased, it is possible that game theoretic approximations to the model can be formed. While the simulations discussed in Sections 4 and 5 are done under biologically feasible parameters, when swimming speed is increased to 100 m d^{-1} and $\varepsilon = 0$, increasingly thin layers for all three models can be exhibited.

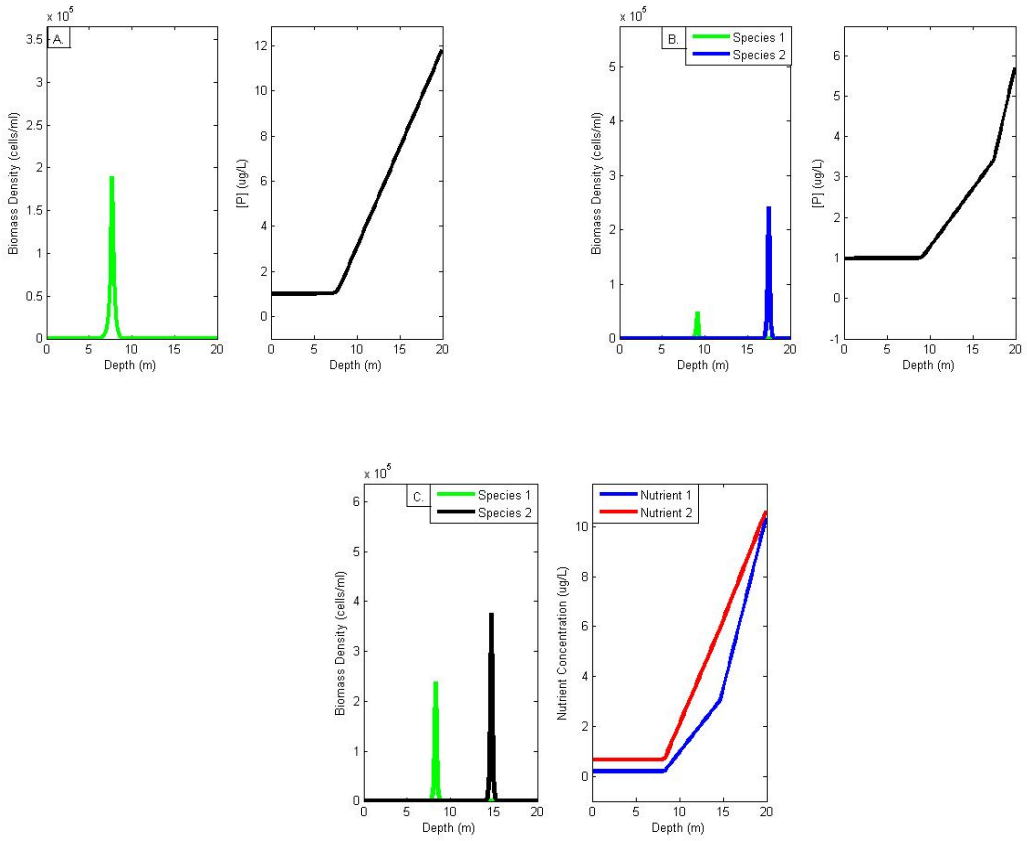

Figure 6.1: Demonstration of increasingly thin biomass layers in all three models.

As outlined in [11], since the phytoplankton are able to form thin layers the competition for light and nutrients can be viewed as a game. The goal is to find a strategy, in this situation a depth, which is evolutionarily stable. A strategy is said to be evolutionarily stable if, when the whole population is using this strategy, any small group of invaders using a different strategy will eventually die off over time [5]. For the single species, the evolutionary stable strategy (ESS) is the depth that

prevents growth in the rest of the water column [11], [14].

To form the game theoretic approximation it is assumed that the phytoplankton can form an infinitely thin layer at a depth z_l by setting $b(z) = B\delta(z_l)$ where $\delta(z_l)$ is the Dirac delta function and B is the total depth-integrated biomass. With this, given a layer at z_l the equilibrium biomass of phytoplankton, the distribution of nutrients, and light in the absence of movement can be calculated. The ESS depth, z^*, is the depth where $g(z) \leq 0$ for $z > z^*$ because either there is insufficient nutrients $R(z) \leq R^*$ or there is insufficient light $I(z) \leq I^*$. The ESS provides a stable equilibrium for the full model [4], [11]. This has been fully developed for the one species and one nutrient model in Section 2. The simulation results for the multi-species models suggest that a similar game theoretic strategy can be developed. To do so, further mathematical analysis of the proposed multi-species models is required. In particular, analysis on existence of solutions and equilibrium distributions is needed for a rigorous treatment.

Finally, to make the model more realistic to use for applications there are a couple of approaches for further model development that can be considered. Since our simulations were concerned with long-term layer formations we ran all simulations with the incident light constant. While it was noted earlier that the model does allow this result to be relaxed, to further increase model accuracy non-constant light should be used. In particular, a light pattern of 15 hours of light and 9 hours of dark would be of considered interest. Additionally, another way the models presented can be modified to more accurately model aquatic ecosystems is to formulate different mathematical schemes for the active movement. For simplifying purposes we assumed all species present in the environment had flagella or cillia so that the active movement can be done by swimming. While this could serve as a first approximation to the movement of a species of practical importance like *Microcystis*, it would be more accurate to have the active movement be modelled as a function of the internal carbon quota of

the cell. This is because *Microcystis* changes the rate at which it conducts photosynthesis to change its buoyancy in the water. Once this task is accomplished it would be of interest to model a two species system where one species' active movement was governed by swimming while the other species' active movement was governed by changing buoyancy.

REFERENCES

[1] Ashino, Ryuichi, Nagase, Michihiro, and Nagase, Vaillancourt, Rémi (2000) *Behind and beyond the MATLAB ODE suite*. Computers & Mathematics with Applications 40: 491-512.

[2] Chattopadhyay, J., Pal, S., and Sarkar, R.R. (2004) *Mathematical modelling of harmful algal blooms supported by experimental findings*. Ecological Complexity 1: 225-235.

[3] Du, Yihong and Hsu, Sze-Bi (2008) *Concentration phenomena in a nonlocal quasilinear problem modelling phytoplankton I: existence*. SIAM Journal of Mathematical Analysis 40-4: 1419-1440.

[4] Du, Yihong and Hsu, Sze-Bi (2008) *Concentration phenomena in a lonlocal quasilinear problem modelling phytoplankton II: limting profile*. SIAM Journal of Mathematical Analysis 40-4: 1441-1470.

[5] Easley, David and Kleinberg, Jon (2010) *Networks, Crowds, and Markets: Reasoning about a Highly Connected World*. Cambridge University Press

[6] Howard, Alan (2001) *Modeling movement patterns of the cyanobacterium Microcystis*. Ecological Applications 11-1: 304-310.

[7] Huisman, Jef and Sommeijer, Ben (2002) *Simulation techniques for the population dynamics of sinking phytoplankton in light-limited environments*. Modelling, Analysis and Simulation: 1-17.

[8] Huisman, Jef and Weissing, Franz J. (1994) *Light-limited growth and competition for light in well-mixed aquatic environments: an elementary model*. Ecology 75-2: 507-520.

[9] Huisman, Jef and Weissing, Franz J. (1995) *Competition for nutrients and light in a mixed water column: a theoretical analysis*. The American Naturalist 146-4: 536-564.

[10] Hutchinson, G.E. (1961) *The paradox of the plankton*. The American Naturalist 95-882: 137-145.

[11] Klausmeier, Christopher A. and Lichtman, Elena (2001) *Algal games: the vertical distribution of phytoplankton in poorly mixed water columns*. Limnology and Oceanography 46-8: 1998-2007.

[12] Krause-Jensen, Dorte, and Sand-Jensen, Kaj (1998) *Light attenuation and photosynthesis of aquatic plant communities*. Limnology and Oceanography 43-3: 396-407.

[13] MacArthur, Robert and Levins, Richard (1964) *Competition, habitat selection, and character displacement in a patchy environmnet*. Proceedings of the National Academy of Sciences (USA) 51: 1207-1210.

[14] Mellard, Jared P., Yoshiyama, Kohei, Lichtman, Elena, Klausmeier, Christopher A. (2011) *The vertical distribution of phytoplankton in stratified water columns*. Journal of Theoretical Biology 269-1: 16-30.

[15] Phillips, O. M. (1973) *The equilibrium and stability of simple marine biological systems I. Primary nutrient consumers*. The American Naturalist 107-953: 73-93.

[16] Reynolds, C.S. (1984) *The ecology of freshwater phytoplankton*. Cambridge University Press.

[17] Rhee, G-Yull and Gotham, Ivan J. (1981) *The effect of environment factors on phytoplankton growth: light and the interactions of light with nitrate limitation*. Limnology and Oceanography 26-4: 649-659.

[18] Smayda, T.J. (1970) *The suspension and sinking of phytoplankton in the sea*. Annual Review of Oceanography and Marine Biology 8: 353-414.

[19] Stewart, Frank M. and Levin, Bruce R. (1973) *Partitioning of resources and the outcome of interspecific competition: a model and some general considerations.* The American Naturalist 107-954: 171-198.